Neuroradiology
https://doi.org/10.1007/s00234-020-02403-1

REVIEW

Radiomics in gliomas: clinical implications of computational modeling and fractal-based analysis

Kevin Jang [1,2] · Carlo Russo [3,4] · Antonio Di Ieva [3,4]

Received: 17 January 2020 / Accepted: 10 March 2020

Abstract

Radiomics is an emerging field that involves extraction and quantification of features from medical images. These data can be mined through computational analysis and models to identify predictive image biomarkers that characterize intra-tumoral dynamics throughout the course of treatment. This is particularly difficult in gliomas, where heterogeneity has been well established at a molecular level as well as visually in conventional imaging. Thus, acquiring clinically useful features remains difficult due to temporal variations in tumor dynamics. Identifying surrogate biomarkers through radiomics may provide a non-invasive means of characterizing biologic activities of gliomas. We present an extensive literature review of radiomics-based analysis, with a particular focus on computational modeling, machine learning, and fractal-based analysis in improving differential diagnosis and predicting clinical outcomes. Novel strategies in extracting quantitative features, segmentation methods, and their clinical applications are producing promising results. Moreover, we provide a detailed summary of the morphometric parameters that have so far been proposed as a means of quantifying imaging characteristics of gliomas. Newly emerging radiomic techniques via machine learning and fractal-based analyses holds considerable potential for improving diagnostic and prognostic accuracy of gliomas.

Key points

- Radiomic features can be mined through computational analysis to produce quantitative imaging biomarkers that characterize intra-tumoral dynamics throughout the course of treatment.
- Surrogate image biomarkers identified through radiomics could enable a non-invasive means of characterizing biologic activities of gliomas.
- With novel analytic algorithms, quantification of morphological or sub-regional tumor features to predict survival outcomes is producing promising results.
- Quantifying intra-tumoral heterogeneity may improve grading and molecular sub-classifications of gliomas.
- Computational fractal-based analysis of gliomas allows geometrical evaluation of tumor irregularities and complexity, leading to novel techniques for tumor segmentation, grading, and therapeutic monitoring.

Keywords Radiomics · Glioma · Computational modeling · Machine learning · Fractal analysis

✉ Antonio Di Ieva
antonio.diieva@mq.edu.au

[1] Discipline of Surgery, Faculty of Medicine and Health, The University of Sydney, Sydney, New South Wales, Australia

[2] Nepean Hospital, Sydney, New South Wales, Australia

[3] Computational NeuroSurgery (CNS) Lab, Department of Clinical Medicine, Faculty of Medicine and Health Sciences, Macquarie University, Sydney, Australia

[4] Department of Clinical Medicine, Faculty of Medicine and Health Sciences, Neurosurgery Unit, Macquarie University, Level 2, Suite 201, 2 Technology Place, Sydney, New South Wales 2109, Australia

Introduction

With the increased research and development of computerized methods to analyze radiological images comes a new frontier for neuroimaging. Beyond qualitative interpretations, methods that incorporate quantitative analyses are changing the way we interpret images. Radiomics is an emerging field that involves extraction and quantification of features from medical images [1, 2]. These data reflect underlying pathological processes and in neuro-oncology can help to improve the understanding of the biology and treatment of brain tumors.

Radiomic features can be mined through computational analysis to produce quantitative imaging biomarkers that characterize intra-tumoral dynamics throughout the course of treatment [3]. This may allow earlier detection of therapy response and subsequent tailoring of treatment to individual patients [2–5].

Glioma is the most common primary brain tumor in adults, representing over 80% of all diagnosed brain tumors [6]. High-grade gliomas (WHO grades III–IV) grow rapidly, infiltrating the brain parenchyma irregularly while creating extensive microvascular networks. Glioblastoma (GBM) carries the worst prognosis of the high-grade gliomas, with a median survival of 12–15 months despite surgery followed by adjunct chemotherapy and radiotherapy [6]. However, survival and response to chemotherapy are incredibly heterogeneous among these patients. This stands in contrast to low-grade gliomas (WHO grades I–II), which are far less aggressive. Traditionally, the management of gliomas was based on their histopathological grade determined by neuropathologists. In recent years, however, specific molecular alterations have been recognized as more prognostic than histological classifications [6]. This has led to an increased understanding of the tumor's genomics, proteomics, and epigenetics as well, and the clinical relevance of these molecular features to therapeutic response and outcome [7, 8]. Modern molecular assessments include isocitrate dehydrogenase (IDH) mutations [9, 10], co-deletion of chromosome arms 1p and 19q (1p/19q) [11, 12], O^6- methylguanine–DNA methyltransferase (MGMT) promoter hypermethylation status [13] and ATRX mutations [14], among others. More recently, gene expression–based molecular characterization of glioma, including epidermal growth factor receptor (EGFR) amplification [15] and CpG island methylator phenotype (CIMP) status have emerged as predictive biomarkers of treatment outcome and response [16]. Both molecular and histological classification, however, require tissue analysis through stereotactic biopsies or resection. These methods are limited by its invasiveness, sampling errors, and interpreter variability [17]. Moreover, there is substantial homogeneity and overlap of imaging features for distinguishing different grades or subtypes of gliomas.

Intra-tumoral heterogeneity is an important hallmark of malignancy associated with poor prognosis. Increased heterogeneity has been linked to increased tumor adaptability, resulting in higher proliferative capacity and survivability leading to higher risk for treatment failure [18]. This is of paramount importance in gliomas, where heterogeneity has been well established at a molecular level as well as visually in conventional imaging [19, 20]. Intra-tumoral heterogeneity interferes with both molecular and histopathological assessments as the analysis of the whole tumor can be challenging. Clonal heterogeneity and genetic variations may be underrepresented in histopathologic sampling leading to sampling errors and suboptimal treatment planning [14]. Radiomics could overcome this limitation by spatially mapping areas of distinct genetic features of the entire tumor [21]. Image-based quantification of molecular heterogeneity could serve as a powerful tool in identifying features that are predictive of response or resistance to therapy [21, 22]. Surrogate imaging biomarkers identified through radiomics could enable a non-invasive means of characterizing biologic activities of gliomas.

In this review, we explore the various features of radiomics-based analysis with a particular focus on computational modeling, machine learning, and fractal-based analysis in improving differential diagnosis and prediction of clinical outcomes and responsiveness to therapy. In doing so, we provide a summary of the morphometric parameters that have so far been proposed as a means of quantifying imaging characteristics of gliomas.

Extracting quantitative image features

Radiomics involves computational methods to reproducibly extract objective, quantitative data from radiologic images [23]. The features are extracted from a defined region of interest (ROI) that includes the whole tumor or specific regions within it. Morphometric parameters are used to quantify visual characteristics at different scales from ROIs, enabling voxel-based analysis of tumor volumetric shapes and visual dynamics. A standard model of radiomics analysis can be seen in Fig. 1. Several approaches to extract radiomic features have been described in the literature, demonstrating accurate methods to capture tumor shape and textural information [24]. Quantitative features can be categorized into the following subgroups: shape features, first-order, second-order, and higher-order statistics features. First-order statistics features describe the distribution of individual voxels regardless of spatial relationships (i.e., histogram-based properties) [25]. Second-order statistics features, generally described as "textural" features, are the statistical inter-relationships between neighboring voxels [25]. This quantifies the spatial distribution of voxel intensities, and thus of intra-tumoral heterogeneity. Higher-order statistics features are extracted by applying filters or mathematical transforms to images; for instance, to identify repetitive or non-repetitive patterns, suppressing noise or highlighting details [25]. An overview of these parameters can be found in Table 1. For their mathematical definitions and detailed explanations, it is suggested to consult the specific literature [24–43].

Although the field of radiomics is progressing at an accelerating rate, it is important to appreciate the historical origins of this complex process. Most of the aforementioned statistical features are neither original nor innovative descriptors [44]. Indeed, the use of basic morphometric features to quantify

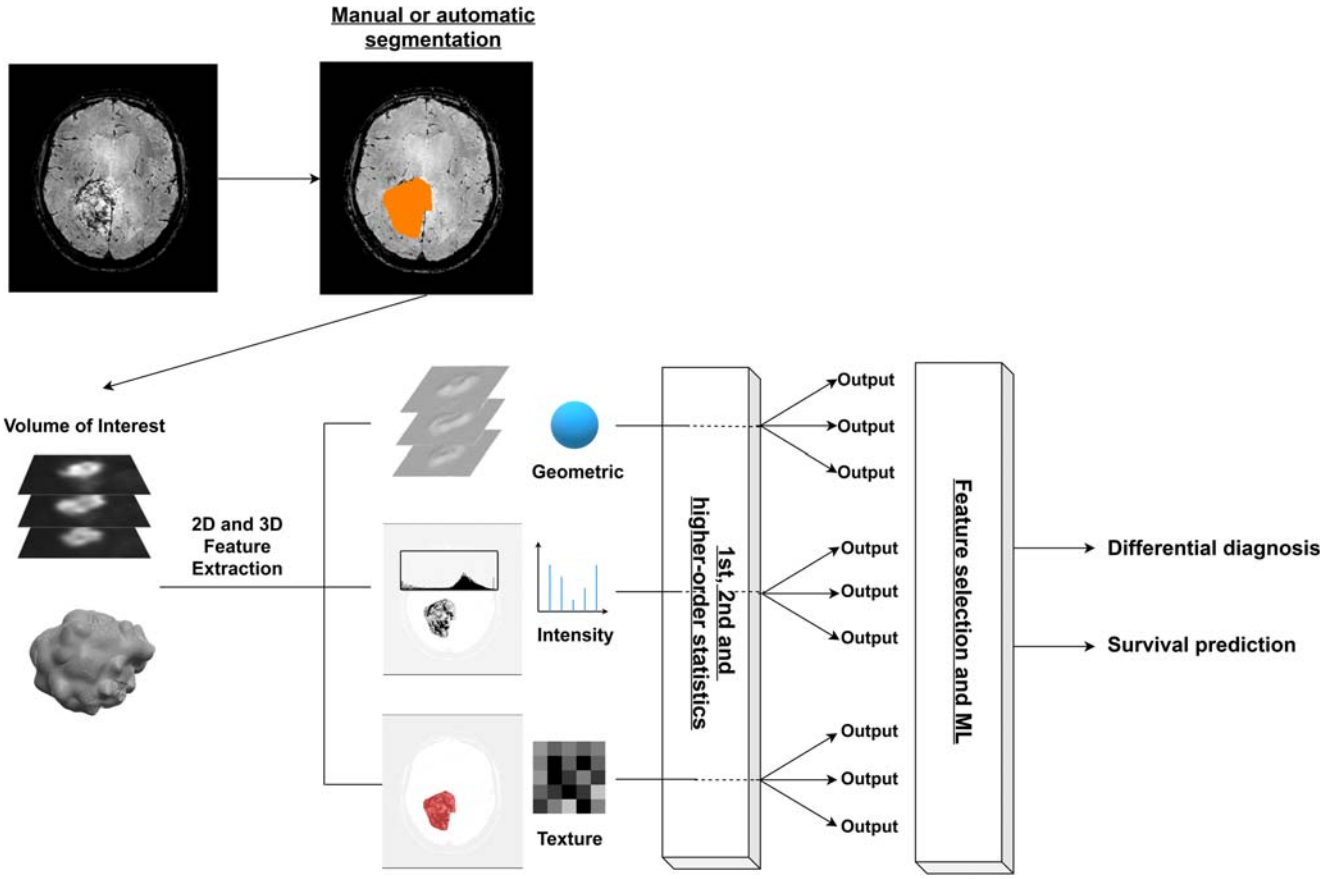

Fig. 1 Flowchart illustrates the standard radiomics workflow and the use of radiomics in clinical decision making. In this example, feature extractions are being performed on a SWI sequence of a segmented brain tumor. The process begins with acquisition of high-quality images. A region of interest (ROI) is identified on these images that contain the whole tumor or sub-regions within the tumor. These are segmented either manually or through automated methods and rendered in three dimensions (3D). Quantitative features are extracted and placed in a database along with other clinical and genomic data. The database is then mined to identify imaging features with the highest diagnostic, prognostic, or predictive value for outcomes of interest

image properties, as well as the use of filters and mathematical transforms, can be traced back several decades in the field of image analysis and engineering [44]. In clinical medicine, one of the first studies to correlate imaging findings with histology was published in 1988 [45]. With no advanced computational techniques, Earnest et al. were able to demonstrate that enhancing regions on images of astrocytomas overlapped with areas of neovascularity and cell proliferation as determined through biopsy [45]. Thus, the novelty of radiomics relies on the –omics suffix, a term originally used for molecular biology disciplines. The term is now used for scientific fields that generate complex high dimensional data from a single source. A key advantage of -omics data is that these data can be mined and extended to generate hypotheses. In clinical imaging, the aim of radiomics is to initially capture as much data as possible and then to use downstream database mining to identify image features with the highest diagnostic and prognostic value.

Despite these recent advances in computational techniques, extraction methods are inherently limited as they distil a complex dataset of over a million voxels per magnetic resonance (MR) imaging sequence down to a relatively small number of quantitative features. In addition, many textural analysis studies still remain on a two-dimensional level (extracting features from a single slice). For a radiomic feature to be reliable, it must fulfill two factors. First, the feature must be able to capture distinct patterns that are associated with improved differential diagnosis and clinical outcomes. And second, the feature must be stable under various image acquisition parameters [46]. Although MR imaging technology has greatly improved in the past decades, linking radiomic features to underlying tissue dynamics has not been fully explored. Indeed, acquiring useful radiomic features becomes increasingly difficult with temporal variations in blood flow and tumor dynamics [47].

In recent years, there has been much effort to develop biologically inspired radiomic features. These features build on biologic hypotheses and can be used to define tissue-level data

Table 1 Parameters used in radiomics-based analysis of gliomas

Parameters and main references	Definition
First-order texture statistics	
Entropy [24]	Measures the inherent randomness in the gray level intensities of an image or ROI.
Uniformity [24]	Measures the homogeneity of gray level intensities within an image or ROI.
Second- and higher order texture statistics	
Gray-level co-occurrence matrix [26]	Examines the spatial distribution of gray level intensities within an image through a 2D gray tone histogram.
Angular second movement [24]	Measures the textural uniformity of an image (also referred to as homogeneity). Captures the two-dimensional complexity of the edge of the tumor abnormalities.
Inverse difference moment [24]	Measures local image homogeneity as it assumes larger values for smaller gray tone differences in pair elements.
Contrast [24]	Measures spatial tone frequency of an image as the difference between the highest and lowest values of a contiguous set of pixels.
Correlation [24]	Measure of gray tone linear dependencies in the image.
Bounding ellipsoid volume ratio [27]	Ratio of the tumor volume to the volume of the smallest ellipsoid that entirely encapsulates the tumor. Captures the three-dimensional complexity of tumors.
Semi-axis diameter ratios [28]	Ratios of the minor semi-axis length to the longest bounding ellipsoid semi-axis diameter. Captures the three-dimensional complexity of tumors.
Margin fluctuation [27, 28]	Captures the two-dimensional complexity of the edge of the tumor abnormalities. Standard deviation of the difference between the ordered radial distances of the tumor edge from the centroid to all the boundary points, smoothed with an averaging filter of length equal to 10% of tumor boundary.
Mean intensity [29]	Average intensity of the pixel values within the ROI.
Mean of positive pixel values [29]	Average pixel values of only the positive pixel values within the ROI.
Standard deviation (SD) [29]	Quantification of the variance from the mean value (high SD indicating wide variation of pixel values).
Kurtosis [29]	Peakedness (or pointedness) of the histogram of pixel values. Positive kurtosis = more peaked distribution Negative kurtosis = flatter distribution
Skewness [29]	Quantifies asymmetry of the histogram. Negative skewness = longer tail on left side of histogram Positive skewness = longer tail on right
Gray-level run matrix (GLRL) [30]	Number of contiguous voxels that have the same gray level value. Characterizes the gray level run lengths of different gray level intensities in any direction.
Short runs emphasis (SRE) [30]	Measures distributions of short runs. Higher values indicate fine textures.
Long runs emphasis (LRE) [30]	Measures distribution of long runs. Higher values indicate course textures.
Gray level non-uniformity (GLN) [30]	Measures the distribution of runs over the gray values. Low value when runs are equally distributed along gray levels. Lower value indicates higher similarity in intensity values.
Run length non-uniformity (RLN) [30]	Measures distribution of runs over run lengths. Low value when runs are equally distributed over run lengths.
Run percentage (RP) [30]	Measures the fraction of the number of realized runs and the maximum number of potential runs. Highly uniform ROI volumes produce a low run percentage.
Neighborhood gray tone difference matrix [31]	One dimensional matrix where each gray level entry is the summation of the differences between all the pixels with gray level value and the average gray level value of its neighborhood.
Coarseness [31]	Quantitative measure of local uniformity.
Busyness [31]	Rapid intensity changes of neighborhoods in a given ROI.
Complexity [31]	Quantifies the complexity of the spatial information present in an image.
Texture strength [31]	Characterizing the visual esthetics of an image.
Local binary pattern (LBP) [32]	Quantifies local pixel structures through a binary coding scheme. Measures tumor microenvironment.
Scale-invariant feature transform (SIFT) [33, 34]	Detects distributed key points with radius on tumor images. Measures tumor spatial characteristics.
Histogram of oriented gradients (HOG) [35]	Computes block-wise histogram gradients with multiple orientations.

Table 1 (continued)

Parameters and main references	Definition
	Measures tumor microenvironment.
Fractal	
Fractal dimension (box-counting and sand-box algorithms) [36–38]	A non-integer number between 0 and 2, in a two-dimensional space, or 0 and 3, in a three-dimensional volume, that quantifies the space-filling properties of irregularly shaped objects.
Outline box dimension [24]	Evaluates the irregularity in shape of the image. (i.e., how much it deviates from classic geometric figures)
Lacunarity [39]	Pixel distribution of an image at different box sizes and at various grid orientations. Describes the degree of non-homogeneity within an image.
Spatial filtering	
Median filter [40]	Reduces sparse noise. Sets each pixel in ROI equal to the median pixel value of its specified neighborhood.
Entropy filter [41]	Accentuates edges by brightening pixels which have dissimilar neighbors. Sets each pixel in the ROI equal to the entropy (measure of disorder) of the pixel values in its specified neighborhood.
Laplacian of Gaussian (LoG) filter [41]	Laplacian filter is a derivative filter used to find areas of rapid change (edges) in an image. Images are first smoothed using Gaussian filter before applying the Laplacian.

variation in tumors. This provides an opportunity to study spatial variations and biologic evolution of tumors [46, 47]. For instance, spatial distances were used to quantitatively measure glioblastoma heterogeneity [48]. Variations in spatial distances within a defined tumor sub-region were associated with distinct prognostic information. In another study, spatial heterogeneity and early temporal changes in regions of high and low perfusion in gliomas were predictive of physiologic responses to radiation therapy [49]. Zhou et al. further proposed a novel concept of extracting quantitative features from distinct tumor sub-regions, such as by their local contrast enhancement, areas of edema, and cellularity in MR imaging [50]. A more recent study also revealed that T2-FLAIR and ADC sequences were inversely proportional to cell density [51]. These novel radiomic features offer an opportunity to quantitatively analyze the tumor environment, unlike the qualitative semantic features commonly used by radiologists to describe lesions.

The importance of image segmentation

Segmentation methods can be broadly categorized into the following: threshold-based, region-based, edge-based, deformable model, machine- and deep learning–based and model-based [52]. A review of these methods can be found in Table 2.

Segmentation is a crucial step of the radiomics process for many reasons. First, data are extracted from the segmented volumes. Moreover, different segmentation methods yield very different geometrical parameters. In gliomas, this is particularly challenging due to their irregular borders. Currently, there is no consensus whether investigators should seek the ground truth or reproducibility of segmentation [1]. Manual segmentation by expert clinicians is often considered the ground truth, despite the high inter-reader variability. This method is also time consuming, labor intensive, and not always feasible for radiomics-based analysis which often requires very large datasets [2]. To this end, automated and semi-automated segmentation methods are being explored to minimize manual input and improve consistency and reproducibility [68]. Whether reproducibility of segmentation outweighs the ground truth remains a controversial topic. Ultimately, however, the validity of any given radiomic feature as a biomarker would have to be assessed on its ability to predict the outcome of interest—i.e., a given molecular, genomic, or clinical endpoint, rather than the "ground truth" as it pertains to the method of segmentation.

Automated and semi-automated segmentation methods have been introduced for various imaging modalities and anatomical regions. Both require maximum automaticity with minimal operator interaction, accuracy, time efficiency, and boundary reproducibility [2]. Certain algorithms use region-growing methods that require an operator to set seed points, thresholds, and iteration termination conditions within the ROI [54]. Although these approaches are effective for relatively homogenous lesions, intensive user correction is often required for lesions that are heterogenous. For instance, gliomas reveal infiltrative growth with lack of clear boundary and fixed growth pattern. Their complex pathological processes can be seen as complex changes in brightness and texture on MR images. Distinct tissues may have similar gray levels, which makes accurate and reproducible segmentation of gliomas challenging [68].

Table 2 Summary of glioma segmentation methods

Segmentation	Method description	Advantages	Disadvantages
Global and local thresholding	Depend on measuring thresholds from the histogram of an image.	Conceptually simple and computationally fast.	Inapplicable to enhancing tumor areas. [53]
Region based			
Region-growing	Begins from a single pixel or group of pixels (seeds). Examines neighboring pixels for similarity and are included to ROI.	Computationally simple. Can correctly segment regions with similar properties and generate connected region. [54]	Partial volume effect limits the accuracy of segmentation. [55] Sensitive to noise or variation in intensity (may result in holes or over-segmentation). Requires manual input for seed selection.
Watershed	Treats pixels as a local topography (elevation). The algorithm floods basin until it reaches the watershed lines, producing a complete contour of images.	Segments multiple regions simultaneously. Produces a complete contour of an image (does not require contour joining). [56]	Over-segmentation.
Edge based	Based on identifying differences between pixels to determine the boundaries of an object.	Computationally fast Does not require prior information about image content. [52] Sensitive to significant variations in gray level values.	Resulting edge does not completely enclose the object. [52] Sensitive to image noise.
Machine learning based			
Supervised	Uses labeled training data.	Can be used for different tasks by simply changing the training set. [52] Can reduce manual engineering task by providing labeled data and appropriate parameters for the learning algorithm. [52]	Requires patient-specific training. [52] Human variability in manually labeling training data.
Unsupervised	Training data are automatically labeled by numerically grouping similar pixels.	Completely automated system.	Number of regions often needs to be pre-specified. [52] Tumors can be divided into multiple regions. [52] Tumors may not have clearly defined textural boundaries. [52]
Fuzzy C means	Unsupervised segmentation by pixel classification.	Unsupervised. Tumor boundaries always converged. [52]	Time consuming. [57] Highly sensitive to noise and heterogeneity.
Artificial neural networks	Supervised clustering method. Extracted features are fed through input nodes, mathematical operations are applied and classification is made as a final output.	Able to model non-trivial distributions and non-linear dependences. [52] Able to learn from historical cases and automatically generate new rules. [58]	Difficulty gathering training samples. [58] Slow learning phase.
Markov random fields	Unsupervised clustering method that integrates spatial information into the clustering process.	Able to represent complex dependencies among data instances. [52]	Difficulty selecting parameters that control the strength of spatial interactions. Requires algorithms that are computationally intensive. [52]
Deep learning based (CNN)			
Interconnected operating modules			
Single path	Unique flow of information: input data is processed; feature maps are mined then used for predicting label in the output layer.	Fast computation and conceptually simple. [59, 60]	Limited parameters. Single flow of information. [59, 60]
Multi-path (parallel)	Composed of different CNNs that work in parallel to capture more comprehensive features. [61]	Able to extract more diverse features. Verdict is validated by interconnected nodules. Included information may provide contextual information to network (e.g., multi-resolution). [59]	Computationally intensive (data preparation and processing). [59]
Multi-path (series)	Different CNNs arranged in a series (cascade) with input from previous network. This makes the overall CNN deeper. [62]	Able to extract even more diverse features.	Requires careful preparation in designing network. [59] Different networks may require training.

Table 2 (continued)

Segmentation	Method description	Advantages	Disadvantages
		Enables refining information at any stage. [59]	Could show minimal improvement.
Input modalities			
Single modality	For processing information from a single imaging modality.	More adaptable to different situations. (e.g., as T1 most commonly provides datasets for tissue and sub-cortical segmentation). [63] Easily used for various modalities.	Single source of information.
Multi-modality	For processing different sources of information from multiple imaging modalities.	Useful for gaining contrast information. [63]	More parameters required than single-modality. [59, 63]
Patch dimension			
2D CNN	Considers features from a single plane (i.e., axial, sagittal or coronal). [60]	Extensible to complex network structures. [59, 60] Flexible and adaptable. Fast computation.	Heavily reliant on initial network design for good results. [59, 60] Excludes 3D nature of MRI.
2.5D CNN (or tri-planar)	Provided with features from the 3 anatomical planes (i.e., axial, sagittal, and coronal), using a multi-path design.	Faster than 3D. Accounts for 3D nature of MRI. Gains implicit contextual information. [64]	Computational more complex than 2D CNN.
3D CNN	Extracts 3D segments directly from the MRI volume. [65]	Able to examine 3D MRI volume directly. [59] Better performance than 2D. Gains implicit contextual information.	Expensive computational cost. Scaling to larger features may be computationally intensive. May require large training data due to large number of parameters (memory requirements). [65]
Number of predictions at a time			
CNN	The traditional approach where a single patch is processed by a network, returning a single output. [59]	In theory, requires far less parameters than FCN.	Time consuming—as a single patch yields a single classification.
Fully convolutional networks (FCN)	The fully connected layers are replaced with a fully convolutional layer—allowing dense pixel-wise prediction. [66]	Quicker segmentation than CNN (some can classify a single volume in one shot). [59, 66]	Requires more parameters to be established. Requires more training samples. May return more false positive predictions when classifying enhancing tumors. [59, 66]
Model-based			
Parametric deformable models (active contour or snake)	Defined by a set of curves of internal and external forces. Internal forces smooth the curves, while external forces change the direction of curves toward the edges of an anatomical area.	Able to extract boundary features for the same regions. Can be used for 3D volumetric segmentation without training data. Able to accommodate for changing biological structures over time. [67]	Depends on user-guidance to place landmarks to steer the segmentation. Sensitive to noise. Requires initializing the contour that is close to the ROI. May converge to wrong boundaries in heterogeneous lesions. [67]
Level sets	Represents contour as the zero-level set of a higher dimensional function, then the method formulates the motion of the contour as the evolution of the level-set function	Accommodates to topological changes. Applicable to volumetric segmentation. [52]	Expensive computational cost.

Routine medical imaging techniques yield a wide variation in acquisition parameters. For MR imaging, these include sequence-type, echo time, repetition time, number of excitations, contrast-enhanced T1-weighted images, diffusion-weighted, and fluid attenuation sequences [44]. Moreover, different manufacturers offer different reconstruction algorithms, and reconstruction parameters are modified at each institution, with possible variations in individual patients. These variables may affect image noise and texture, and consequently the quality (and reproducibility) of the radiomic features. In a given T1- or T2-weighted sequence, no voxel intensity carries a fixed tissue-specific numerical value [44]. It is important to consider that some acquisition settings may yield unstable features, which may produce different values

when extracted under identical conditions. For instance, even when scanning the same patient in the same position using the same scanner with the same sequence over multiple sessions, signal intensity may change, whereas tissue contrast remains unaffected [69]. These limitations must be considered when comparing radiomic features among patients as the process relies on the numeric value of voxel intensity. One method could be to perform textural analysis on features quantifying the relationship between voxel intensities, not requiring values of individual voxel intensity, or through image compensation (normalization) before performing quantitative analysis [69], such as the Brightness Progressive Normalization algorithm, introduced by Russo C and published first by Di Ieva et al. in 2012 [70].

Clinical application of radiomics

Survival prediction

The survival prediction according to radiological features remains a challenge in gliomas, above all in glioblastoma, due to intra-tumoral heterogeneity. A recent genomic analysis by Sottoriva et al. revealed extensive intra-tumor variability at molecular, cellular, and tissue scales [71]. However, the clinical relevance of the spatial imaging characteristics remains enigmatic. Stratifying accurate prognosis of survival using radiomic spatial features pushes gliomas closer to the paradigm of precision medicine. With novel analytic algorithms, quantification of morphological or sub-regional tumor features to predict survival outcomes has produced promising results. Recent progress in the clinical application of radiomics is summarized in Table 3.

Morphometric analysis: shape, texture, and volume

There is paucity of evidence on computational image analysis of tumor morphology and its prognostic implications. Prior studies often used 2D or simple 3D features such as tumor volume, with no control for prognostic variables, such as the Karnofsky Performance Score (KPS) or patient age. To overcome this shortcoming, Czarnek et al. demonstrated that after controlling for these variables, algorithmic analysis of GBM shapes was significantly prognostic of survival [27]. Using automated tumor segmentation from FLAIR sequences, three morphological features were found to be independently prognostic of survival ($p < 0.05$): (a) glioma bounding ellipsoid volume ratio, (b) margin fluctuation, and (c) angular standard deviation. On FLAIR alone, margin fluctuation and angular standard deviation were not statistically significant for prognosis; however, when analyzed with post-contrast T1-weighted MR images, both of these features were significant for survival prediction [27]. Thus, this proves the importance of analyzing multimodal parameters and the vast amount of information we can deduct from clinical imaging to shape our clinical practice.

Similarly, in a recent retrospective study, Molina et al. revealed the predictive potential of 3D textural heterogeneity of GBMs in post-contrast T1-weighted MR images [74]. Textural features were quantified as spatial distribution of voxel intensities, allowing visualization of heterogeneity patterns within the segmented ROI of the tumor. These parameters were classified as local (co-occurrence matrixes [CM]), regional (run-length matrices [RLM]), or global (voxel intensity histograms). High parametric values describing tumor homogeneity were associated with longer survival groups, while high values in heterogeneity were associated with poor survival [74]. This produced a threshold for classifying subset of patients into long- and short-term survivors, which may ultimately guide patient selection for surgical resection.

With the rise of machine learning in clinical medicine, predicting overall survival in GBM patients has reached a new frontier. Sanghani et al. analyzed tumor volumetric, shape, and texture features from multiple MR images to predict overall survival of patients using machine learning techniques [76]. Survival groups were defined as short (< 10 months), medium (10–15 months), and long (> 15 months). Using a support vector machine (SVM) classification for feature selection, the morphological features were stratified into two groups—2-class (< 400 days and > 400 days) and 3-class (short, medium, and long as defined above) survival group prediction. The feature selection and prediction framework produced high accuracy for both classes in predicting overall survival, where 2-class classification yielded 97.5% and 3-class yielded 87.1%. These results testify to the power of radiomics in predicting disease prognosis, thus providing invaluable information for tailoring treatment plans to individual patients.

Sub-regional variability

Several studies have demonstrated that GBM heterogeneity is not only limited to tumor margins but also involves peritumoral brain parenchyma tissue. Analysis of these regions and its microenvironment suggests cellular and molecular interaction that contributes to tumor infiltration, breakdown of blood brain barrier, and microvascular proliferation, ultimately leading to poorer prognosis [79]. Radiomics allows one to study these subtle macro- and micro-scale changes within the lesion through quantitative measurement. The clinical relevance of these micro-architectural changes stands on two principal hypotheses: (a) radiomic features derived from multiparametric MRI sequences can reveal subtle quantitative traits associated with tumor aggressiveness, and (b) these traits are distinct between long- and short-term GBM survivors [79].

Table 3 Major developments in radiomics modeling for gliomas

Author (year)	Study population	Study methodology	Major findings
Georgiadis et al. (2009) [72]	67	1. Volume of interest (VOI) segmented from MRI series. 2. Volumetric textural features extracted (gray-level co-occurrence and run-length matrices). 3. Bagging (bootstrap aggregation) of 3 LSFT-SVMs for classification scheme.	3D volumetric textural analysis improved discrimination accuracy between metastases, gliomas and meningiomas. Modified support vector machine (SVM) classifier using least square features transformation (LSFT) improved discrimination accuracy.
Zhou et al. (2014) [50]	32	1. Linear normalization of tumor region. 2. Manual segmentation of ROI on T1+C. 3. 2D and 3D histogram analysis.	Long-term survival group had tumor habitats with high enhancement and high cell density. Poor survival group had tumors with increased regions of low enhancement.
Yang et al. (2015) [73]	82	1. Tumor regions manually segmented T1-w and FLAIR MR images. 2. 5 sets of textural features extracted: segmentation-based fractal texture analysis, histogram of oriented gradients, run-length matrix, local binary patterns, Haralick features. 3. Ensemble classifier (random forest) used to predict GBM molecular subtype and 12-month survival status.	Textural features are predictive of molecular subtypes and survival status in GBM.
Zhou et al. (2013) [48]	16	1. Image data acquisition. 2. Tumor region identification. 3. Data normalization. 4. Image segmentation with OTSU algorithm. 5. Distance between two segmented regions measured.	Slow progression (> 500 days)—smaller distances between ROI compared with fast progression.
Zhou et al. (2017) [3]	32	1. Pair of tumor MRI slices selected as inputs. 2. Each sequence segmented by OTSU. 3. Tumor region separated into two sub-regions. 4. Spatial mapping to impose an overlap between segmented sequences. 5. Features extracted from contrast-enhanced regions given to machine-learning algorithm to build classifier to predict survival.	Spatial characteristics derived from tumor sub-regions of edema (T2 and FLAIR) had the highest predictive value of prognosis (81.25% accuracy).
Molina et al. (2016) [74]	79	1. Semi-automated image segmentation. 2. Segmented image manually corrected. 3. 16 heterogeneity measures computed automatically. 4. Run-length matrix features used for regional heterogeneity. 5. Co-occurrence matrix features used for local heterogeneity.	3D textural heterogeneity measures computed on post-contrast T1 MRI are predictors of survival.
Chang et al. (2016) [75]	126	1. Volumetric tumor segmentation 2. Image registration, normalization and ADC submask generation. 3. Imaging features extraction: histogram, shape, multimodal parametric and textural. 4. Machine learning algorithm generated. 5. Kaplan-Meier analysis to evaluate progression-free survival and overall survival.	Machine learning techniques to analyze multimodal imaging features could accurately predict survival in patients with recurrent glioblastoma treated with bevacizumab.
Gutman et al. (2013) [4]	75	1. Pre-surgical MR images interpreted by 3 neuroradiologists for size, location and morphology using standardized feature set. 2. Inter-rater analysis performed using Krippendorff α statistic and intra-class correlation coefficient. 3. Multivariate Cox regression models for association between survival and tumor size/morphology. 4. Fisher exact test for relationship between imaging features and genomics.	Overall survival was highly correlated to degree of contrast enhancement and length of major axis of lesion. A semiquantitative computed method using standardized visual feature set improved estimation of contrast enhancement.
Czarnek et al. (2017) [27]	68	1. Five shape features automatically extracted from manually segmented tumor regions. 2. 3D features: nearest neighbor interpolation between MRI slices to reconstruct 3D tumor shape. Fitted smallest	Algorithmic 3D analysis of tumor shape is a strong prognostic marker of survival independent of patient age, Karnofsky Performance Score and tumor volume.

Table 3 (continued)

Author (year)	Study population	Study methodology	Major findings
		bounding ellipsoid to the 3D tumor shape based on Khachiyan algorithm. 3. 2D features: extracted from axial FLAIR and T1+C images with largest tumor cross-section. Measured margin fluctuation and angular standard deviation.	
Mazurowski et al. (2016) [28]	22	1. Manual segmentation of pre-operative axial FLAIR images. 2. Extracted set of 5 features using computer algorithms. 3. 2D features: margin fluctuation and angular standard deviation were calculated. 4. 3D features: minimum bounding ellipsoid ratio, semi-axis diameter ratios.	The proportion of the tumor volume to the volume of the smallest bounding ellipsoid is strongly predictive of patient survival.
Sanghani et al. (2018) [76]	163	1. Volumetric, shape and texture features extracted from regions of edema, contrast-enhancement and necrosis. 2. Feature selection using recursive feature elimination (RFE). 3. Linear support vector machine (SVM) used for survival group prediction.	Overall survival can be predicted with high accuracy using machine learning to analyze tumor volumetric, shape and texture features.
Lao et al. (2017) [77]	112	1. Segmentation of tumor sub-regions: necrosis, enhancement and edema. 2. Handcrafted features extracted: geometry, intensity and texture. 3. Deep features extracted from pre-trained CNN model via transfer learning. 4. Four-step feature selection. Six most predictive deep features selected. 5. Radiomics signature and radiomics nomogram constructed.	Deep learning–based radiomics model can accurately predict overall survival by stratifying patients into high and low-risk groups. Radiomic signatures identified through deep learning outperformed manual extraction.
Li et al. (2017) [78]	92	1. Image pre-processed then automatically segmented into 5 classes: non-tumor region and 4 tumor sub-regions (necrosis, edema, enhancing and non-enhancing area). 2. High-throughput radiomics features extracted from tumor sub-regions. 3. Feature reproducibility and prognostic performance assessed.	Introduced a fully automatic multiparametric radiomics model for pre-operative prediction of overall survival in GBM patients. Multiparametric radiomics signature offered better prognostic performance than fixed-parameter signatures.
Prasanna et al. (2017) [79]	65	1. Image pre-processing and registration. T2-w and FLAIR were co-registered with T1+C. 2. Segmentation of tumor into 3 regions: parenchymal zone, necrosis and enhancement. 3. 134 radiomic features obtained, resulting in 9 feature sets. 4. Identified 10 most predictive features. 5. Random forest classifier used to determine ability of each feature set in predicting survival groups. 6. Randomized 3-fold cross-validation performed. 7. Kaplan-Meier survival analysis used to compare survival times between short and long-term survivors.	Peri-tumoral radiomic features outperformed features from other regions (enhancing, necrosis) in predicting survival. Peri-tumoral radiomic features combined with clinical features (age, KPS) were more predictive of survival than radiomic features alone.
Bahrami et al. (2018) [80]	33	1. Volumes of interest (VOI) within FLAIR hyperintense region were segmented. 2. Edge-contrast for each VOI was calculated using gradients of 3D FLAIR images. 3. Cox proportional hazard models were used to determine relationship between edge contrast and progression-free/overall survival. Age and extent of surgical resection were used as covariates.	Texture analysis using edge-contrast of FLAIR hyperintense regions may be predictive of survival in high-grade gliomas treated with bevacizumab. Low edge-contrast (vague borders) has poorer progression-free survival and overall survival compared with patients with high edge-contrast (sharp border).
Bisdas et al. (2018) [81]	37	1. DKI acquired using spin-echo echo planar imaging DWI sequence. 2. Tumor VOIs manually segmented around FLAIR abnormality. 3. Texture features extracted from both DKI and FLAIR VOIs.	Diffusional kurtosis imaging (DKI) accurately predicts IDH mutational status. Texture analysis and SVM analysis of DKI maps produced biomarkers to distinguish IDH-mutant from IDH-wildtype as well as grade II from grade III gliomas.

Table 3 (continued)

Author (year)	Study population	Study methodology	Major findings
		4. SVM analysis for binary classification: glioma grading and IDH mutation status. 5. Biomarker selection using recursive feature elimination.	
Bae et al. (2018) [82]	217	1. Radiomic features extracted from multiparametric MRI. 2. Random survival forest model trained with radiomic features along with clinical and genetic profiles. 3. Incremental values of radiomic features assessed using integrated area under the receiver operating characteristic curve.	Radiomic phenotyping based on multiparametric MRI data improves survival prediction when integrated with clinical and genetic status in patients with GBM.
Bahrami et al. (2018) [83]	61	1. Patients with grade II/III gliomas with molecular data and MRI prior to radiation included. 2. Quantitative MRI features extracted—tissue heterogeneity (homogeneity and pixel correlation) and FLAIR border distinctiveness (edge contrast). 3. *T* tests performed to determine whether patients with different genotypes differed across the features. 4. Logistic regression with LASSO regularization used to determine optimal combination of imaging and clinical features for predicting molecular subtypes.	Quantitative FLAIR textural features (signal heterogeneity and border sharpness) may serve as a useful imaging biomarker for determining tumor molecular status in grade II/III gliomas.
Chaddad et al. (2018) [84]	40	1. Acquisition of pre-treatment MR images. 2. Registration of T1-w image with corresponding FLAIR images and labelling of GBM subtypes (phenotype). 3. Multiscale texture feature extraction. 4. Survival analysis.	Using Laplacian-of Gaussian (LoG) filter to generate multiscale texture features has the potential to predict GBM survival.
Ditmer et al. (2018) [29]	94	1. ROI manually segmented on T1+C images. 2. Textural analysis performed using filtration-histogram method. 3. Parameters were correlated with WHO glioma grade using Spearman correlation. 4. AUC calculated using ROC curve analysis to distinguish tumor grades.	Quantitative measurement of heterogeneity using MRI textural analysis can accurately discriminate high versus low grade gliomas.
Darbar et al. (2018) [85]	48	1. ADC values calculated in areas of greatest restriction in solid tumor components. 2. Pattern of contrast enhancement recorded. 3. ROC analysis used to evaluate predictive potential of ADC values for low grade gliomas.	ADC of tumor regions on pre-operative MRI can discriminate high- and low-grade gliomas. Low grade gliomas have significantly higher mean lowest ADCs than high grade gliomas.
Osman A (2019) [86]	163	1. Radiomic image features extracted locally from 3 tumor sub-regions on multi-parametric MR images. 2. LASSO regression applied for feature selection. 3. Radiomic signature model of 9 features constructed. 4. Model tested for patient stratification into short (< 10 months), medium (10–15 months) and long survivors (> 15 months). 5. ML classification models trained then cross-validated.	A derived gray-level co-occurrence matrix feature was found to be highly associated with survival—suggesting intra-tumoral heterogeneity has an essential role in survival stratification. Ensemble learning showed superior performance over the tested ML classifiers.
Petrujkić et al. (2019) [87]	55	1. Each tumor outlined on T1+C images. 2. ROI over imposed to corresponding T2-w and SWI images. 3. Tumor representation in these 3 sequences were segmented. 4. Binary image obtained. 5. Quantitative parameters of fractal and texture analysis were estimated—using box-counting method and GLCM methods.	Textural features are more significant than fractal-based features in differentiating glioblastoma from solitary metastasis.
Yang et al. (2019) [88]		1. Textural features from 30 parametric maps were extracted using 4 models: global, GLCM, GLRLM, GLSZM. 2. These features were then input into RBF-SVM combined with attribute selection using SVM-RFE. 3. SVM model was trained and established using 10-fold cross validation.	Gray-level size-zone matrix (GLSZM) combined with gray-level 64 may be the optimal texture retrieving model for glioma grading.

In a recent experimental study, Zhou et al. identified quantitative spatial imaging biomarkers with prognostic value in predicting survival outcomes [3]. Through two datasets of patients with unresected GBM, tumor habitats were quantified on multiple MRI slices (including contrast-enhanced T1, FLAIR, and T2 sequences). Quantitative features from signal enhancing tumor sub-regions revealed discriminative ability in predicting survival groups. More specifically, spatial characteristics derived from sub-regions of edema (co-occurring MRI signals in FLAIR and T2-weighted images) displayed the highest predictive ability in separating long-term (> 400 days) and short-term (< 400 days) survival groups. Mapping sub-regions of edema yielded the highest accuracy of 81.25% in predicting survival groups ($p < 0.05$)—indicating strong prognostic value of MRI-defined sub-regions in GBMs.

With the same fundamental concepts, Lao et al. developed a deep learning–based radiomics model to predict survival outcomes in GBM patients [77]. Three tumor sub-regions were segmented from multimodality MR images (T1, post-contrast T1, T2, and FLAIR), including areas of necrosis, enhancement, and edema. Handcrafted and higher-order deep features were then extracted for selection, with the final aim of selecting features with prognostic value. A six-feature radiomics signature was constructed, and these signatures were shown to accurately stratify 75 patients into high- and low-risk groups, successfully predicting overall survival. All six features were deep features derived from multiple tumor sub-regions in post-contrast T1, T2, and FLAIR images. It is not surprising that deep features extracted via transfer learning outperformed traditional manual extraction in predicting overall survival—as higher-order imaging patterns can capture more intra-tumoral heterogeneity [77]. Such radiographic heterogeneity of GBMs may reflect underlying genetic heterogeneity, which could explain treatment resistance and poorer prognosis. However, this remains a complex hypothesis and defining the correlation between deep features and genetic characteristics requires further research. Despite the study being retrospective with a relatively small sample size, the proposed radiomics model has the potential to shape preoperative management of patients with GBM.

Prasanna et al. similarly extracted radiomic features from sub-regions of GBM habitat including enhancing tumors, necrotic areas, and the peri-tumoral brain parenchyma zones [79]. These features were derived from 65 pre-treatment multiparametric MRI sequences (T1, T2, and FLAIR) in order to distinguish long- and short-term survivors. Peri-tumoral features were found to be more predictive across T2 and FLAIR ($p = 0.0006$ and $p = 0.003$, respectively) compared with enhancing areas or necrotic features. However, on post-contrast T1, radiomic features from necrotic sub-regions were more predictive of survival prognosis than peri-tumoral zones ($p = 0.006$). Interestingly, when peri-tumoral features were combined across multiparametric sequences, it revealed higher predictive ability than radiomic features derived from necrotic or enhancing areas. This result is reflected in other studies that have demonstrated peri-tumoral edema on MRI as a negative prognostic marker; however, the precise role of peri-tumoral brain parenchyma zones in GBM prognosis remains controversial. For instance, in a multi-institutional study by Schoenegger et al., surrounding areas of edema were identified as an independent prognostic marker, where patients displaying extensive edema had significantly poorer overall survival compared with those with minimal edema [89]. However, this finding was contradicted by Lacroix et al. in a large series of 416 GBM patients where the extent of edema was not a prognostic marker for overall survival [90]. Thus, the prognostic implications of peri-tumoral edema in GBM have been inconclusive in the literature. The reason for these inconsistencies may be due to prior studies only examining gross volumetric measurement of these areas. Radiomics holds the potential to overcome these limitations through capturing subtle local variations in image intensities that are otherwise visually not appreciable.

Classification of glioma subtypes

The relationship between intra-tumoral heterogeneity and tumor infiltrative capacity, response to treatment and overall survival has been well established in the literature. Although the current gold standard for grading gliomas involves histopathological analysis, stereotactic biopsies, or resection, these techniques are inherently limited by its invasiveness, sampling error, and interpreter variability [17]. Moreover, there is significant overlap of conventional and multiparametric imaging features for differentiating high- and low-grade tumors. Thus, radiomic analysis to quantify intra-tumoral heterogeneity may improve diagnostic and prognostic accuracy allowing tailored treatment planning and monitoring of therapeutic response.

As mentioned previously, textural analysis is a key tool of radiomics in unraveling complex imaging patterns. Algorithms can examine spatial distribution of gray levels in an image, by incorporating a filtration-histogram approach where textural features of varying intensities are quantified using histogram-based statistical metrics [29]. Several studies suggest that these extracted features may be of potential use as spatial imaging biomarkers for GBM heterogeneity. This is exemplified by a recent study by Skogen et al., where histogram-based textural analysis of GBM on MR images was able to accurately discriminate high- and low-grade tumors [91]. Ditmer et al. further extended this notion through a retrospective study of 94 patients to determine the accuracy of radiomic-based filtration-histogram textural analysis in grading gliomas [29]. Their analysis found that fine texture features on post-contrast T1 images have the strongest ability in discriminating high- and low-grade gliomas. This reiterates

the findings by Skogen et al. where fine texture scales were also found to be the best discriminative feature, with a sensitivity and specificity of 93% and 81% ($p < 0.05$) [29].

Despite the accumulating work in improving differentiation of gliomas through radiomic models, there remains a question of adding value to molecular sub-classifications. To address this, Macyszyn et al. applied machine learning and pattern recognition methods to predict GBM molecular subtypes by extracting imaging phenotypes [92]. Tumors were categorized into four subtypes through an isoform-level assay classifier: (a) proneural, (b) neural, (c) mesenchymal, and (d) classical. Molecular subtypes were predicted with an overall accuracy of 75.76%. Imaging phenotypes that were most predictive for each subtype were (a) histogram of T2-FLAIR intensity and mean T1 in enhancing tumors for proneural subtype, (b) T2 intensity histogram in areas of edema and tumor location for neural subtype, (c) histogram of T2-FLAIR intensity and mean T1 signal in edema for proneural subtype, and (d) size of enhancing regions, T2-FLAIR intensity histogram, and peak height on perfusion signals in areas of edema for classical subtype. Several studies have shown similar findings where specific molecular subtypes of GBM displayed unique imaging phenotypes that could be extracted and used as non-invasive biomarkers. For instance, mesenchymal tumors have been found to have lower non-enhancing tumor volume and surrounding edema intensity, proneural subtypes have significantly lower blood-brain barrier breakdown, and classical subtypes are strongly associated with features of necrosis and edema [92]. Unlike prior studies that involved tissue specimen analysis, Macyszyn et al. demonstrated that molecular subtypes of GBM can be accurately predicted using imaging alone.

Computational fractal-based analysis

The application of fractalomics in neuroscience is relatively a new paradigm [37, 38]. Fractal analysis is a tool used to mathematically assess morphological features (e.g., roughness and geometrical complexity) of natural objects [37, 38]. Within the last decade, fractal analysis has become an attractive method to quantify complex morphological features in computed tomography (CT) and magnetic resonance imaging [38]. More recently, it has been applied in neuroimaging for automated classifications to improve diagnostic and prognostic accuracy [93–95]. Fractal dimension, a parameter used in fractal analysis, is a non-integer number between 0 and 2, in a two-dimensional space, or 0 and 3, in a volume of interest, that quantifies the geometrical complexity of natural objects and their ability to fill the surrounding space in which it is embedded [38]. Fractal dimension computation has been shown to be useful in characterizing the complex morphology of the brain cortex, thus suitable to distinguish pathophysiological states in MR imaging [38].

Several experimental studies have used fractal analysis for MR brain imaging classifications, given its unique ability to evaluate the self-affinity at multiple scales and the long-range correlations of an image [38]. Authors have hypothesized that normal brain MRI has higher self-affinity and long-range correlations compared with those with neuropathologies, and that these morphological changes can be quantified using computational fractal-based analysis [38, 93–95]. For further details regarding the theoretical principles of fractal-based analysis and its clinical applications into the basic and clinical neurosciences, see Di Ieva et al., references [37, 38, 96].

Fractal geometry of brain tumors

The geometrical structure of tumors tends to be complex and irregular due to the uneven spatial distribution of their cells and microvessels. In particular, brain tumors exhibit irregular geometry during their growth process and are apparent even in their microvascular networks and spatial diffusion through time. Fractal-based analysis in neuroimaging has been fundamental in the geometrical evaluation and quantification of tumor irregularities. Its precise ability to characterize geometric features of irregular and complex natural objects has led to novel techniques for tumor segmentation [58, 97, 98], tumor grading [97, 99], and therapeutic monitoring [70, 97]. Parameters computed by means of fractal analysis can be used to not only validate tumor growth models but also to gain further clinical and prognostic information in oncological patients [100].

Fractal-based parameters, such as the fractal dimension (FD), have been increasingly used for tumor segmentation in neuroimaging, oncologic grading, and evaluation of therapy [101]. More specifically, MRI with contrast enhancement [97], susceptibility-weighted MRI (known as SWI) [70, 99], and histological specimens have been assessed by means of fractal analysis [102–106]. For instance, Di Ieva et al. evaluated the fractal dimension on 7 Tesla SWI-MRI for grading of gliomas [99]. Their findings revealed an increasing trend of the intra-tumoral SWI patterns' fractal dimension with tumor grade—1.682 ± 0.278 for grade II, 2.018 ± 0.517 for grade III, and 2.247 ± 0.358 for grade IV gliomas. Statistically significant difference was found between grade II and grade IV gliomas ($p < 0.05$), which proved that fractal geometric analysis can accurately distinguish high- and low-grade tumor. In an earlier study, fractal capacity dimension was used to evaluate the effects of antiangiogenic treatments [70]. This was also performed on 7 Tesla SWI-MR images to monitor in vivo the therapeutic response. These promising results testify to the value of using fractal analysis on 7 T SWI-MRI to quantitatively examine malignant brain tumors and their dynamics during antiangiogenic therapy.

Fractal geometry analysis on post-contrast MR images has also been applied by Iftekharuddin et al. [58, 97] and Zook et al. [98] for brain tumor detection and FD estimation. They proposed three modified box-counting algorithms where pixel intensities can be viewed in the third dimension, rendering them more suitable for fractal textural analysis. Using a feature extraction methodology with a self-organizing map, multiple fractal parameters were derived from post-contrast T1, T2, and FLAIR MRI modalities. Following this extraction, the authors could train a supervised neural network to automatically classify image regions as tumorous or non-tumorous. Several authors have also used FD to analyze the 3D tumor interface in GBMs. Interestingly, Smitha et al. analyzed FLAIR sequences to assess variations in fractal dimensions of the tumor contours in low- and high-grade gliomas [39]. Low-grade gliomas yielded a FD of 1.243 ± 0.127, while high-grade gliomas revealed 1.338 ± 0.248, with a statistically significant difference ($p < 0.05$).

A dataset of fractal dimensions correlates to a particular feature of the brain tumor lesion, such as enhancing regions, geometric texture, vascularity, and tumor interface. These features are invaluable in characterizing the dynamic evolution of brain tissue from normal to dysplastic and to neoplastic. Such descriptors may greatly contribute to improving diagnosis and therapeutic monitoring, and serve as the platform for developing innovative tumor growth models for optimizing therapy and drug delivery.

Future perspectives

Substantial progress has been made in the field of radiomics to improve our understanding of the biology and evolution of brain tumors. Quantitative characteristics derived from neuroimaging modalities enables imaging surrogate biomarkers to be validated through machine learning and fractal-based analyses. This allows subtle variations in the intra-tumoral microenvironment to be monitored throughout the course of treatment. Despite the growing body of literature, there remains a need to develop more specific and precise methods to apply quantitative imaging features in a clinical setting. Here, we explore the challenges and opportunities that pertain to brain cancer imaging and the application of radiomics in neuro-oncology.

The role of big data

Modern healthcare has seen an exponential growth in biomedical data generation and extraction from individual patients [1]. Massive datasets, so-called "big data," are required by radiomic studies to validate deep learning–based approaches and expand its clinical applications [107, 108]. Despite the growing potential for radiomics, there remain logistical and technical challenges in managing big data. With multiple data sources (e.g., institutions) and various data types (e.g., multiparametric imaging data, gene expression profiles, and clinical records), standardizing data collection and sharing become incredibly complex [46]. Differences in image acquisition and reconstruction are covariates that must be addressed in the mining of quantitative features. Standards will have to be established across different image protocols and parameters to validate results from radiomic models. Thus, there is a need for mutual agreements between national, international, and multi-institutional consortia to share data through centralized or federated networks [1]. Initiatives such as The Cancer Genome Atlas [109], The Cancer Imaging Archive [110], and the Quantitative Imaging Network [111] have allowed efficient sharing of clinical data and help validate imaging biomarkers against an independent dataset. However, establishing high-quality benchmarks with complete clinical labels, standard radiomic features, and molecular profiles remains to be challenging at a larger scale. Growing efforts to improve data sharing, experimental evaluation, and reproducibility will push radiomics closer toward precision medicine.

The role of radiologists

In current practice, radiologic investigations are qualitatively examined. The finalized reports often do not use a standard lexicon, despite recent efforts such as the RadLex® [112]. Although guidelines exist for reporting, none are available for reporting quantitative imaging features, let alone for reporting highly complex radiomics features. Due to the lack of standards, huge existing image repositories are essentially inaccessible for curation. Moreover, archived medical images are rarely re-accessed. The most practical solution would be to capture data prospectively at the point of care. This may lead to a transition from classic radiology to a future where radiologists actively participate in the curation of quantitative image databases [1]. Generating high-quality image data would require considerable expertise in identifying, segmenting (with computer assistance), and annotating (using a standardized and mineable lexicon) the regions of interest [1]. For the curation of high-dimensional data to become a reality, radiologists should be first convinced of its value, and the process must be refined to work within the limitations of clinical practice. Indeed, we envision radiomics to become a valuable asset to improving diagnostic accuracy and clinical decision making. With further involvement of radiologists in the curation and analysis of big data, radiomics will continue to push the boundaries of precision medicine.

Developments in machine learning

As described previously, identifying multiparametric prognostic imaging biomarkers remains a challenge when extracting

large-scale radiomic features from numerous imaging modalities. Development of machine learning algorithms to analyze rich databases could prove to be beneficial in identifying clinically relevant feature descriptors [46]. Sparse-learning models, also referred to as lasso regularization [113], have been used in other cancer pathologies to identify prognostic imaging biomarkers—such as non-small cell lung cancer [114]. Although its applicability in neuroimaging is still lacking, recent developments in SVM learning and deep learning models prove to be encouraging in classifying GBM subtypes. However, the lack of widely available labeled medical data poses a challenge for developing novel deep learning models [46]. For instance, collecting a large enough database of cancer images with accurate histopathological labels is costly at scale; thus, developing methods to integrate data with varying clinical labels may provide the opportunity to input large datasets for deep learning models [115]. The clinical relevance of deep learning outputs from multi-scale medical data (e.g., multimodal MR imaging and genomics) remains uncertain; however, the ability to extract concise imaging patterns via artificial neural networks may guide future studies in developing large-scale radiomic models [116].

Developments in targeted therapy

Optimizing treatment selection for GBM requires further research into developing specific radiomic signatures. With neuroimaging modalities such as diffusion-weighted sequences, there is growing evidence that ADC maps may be beneficial to differentiate clinical outcomes in GBM treated with radiation therapy concurrently with temozolomide [117]. In fact, early variations in ADC maps were identified as a potential marker for predicting GBM recurrence [118]. As mentioned earlier, machine learning and fractal-based analyses were also used to predict treatment responses to bevacizumab—where a decrease in the volume of FLAIR signal and contrast enhancement was found as a potential biomarker in estimating therapeutic success [119]. To further improve our understanding of intra-tumoral dynamics expressed as imaging phenotypes, larger collection of radiomic features extracted at various diagnostic periods could provide an opportunity to describe tumor evolution before and after treatment [120]. Distinguishing tumor growth between pseudo-progression and pseudo-response continues to be a challenge through imaging alone [121]; thus, development of radiomic models to better characterize treatment outcomes will push the field of neuro-oncology a step closer to precision medicine. Although validation of radiomic features as true predictors of treatment response is yet to be defined, the growing depth of radiomic findings combined with growing genomic and clinical data may provide the opportunity to redefine our understanding of GBM biology. In the coming years, radiomic analysis, using fractal geometry or higher-order statistical methods such as machine learning or deep learning, will be eventually able to redefine tumor subtypes paving way for discovery of new biomarkers, with the final aim to improve decision making and patients' treatment.

Developments in fractal analysis

In regard to fractal-based analysis, its efficacy in classifying brain MR images has been well established through many breakthrough studies in the field of biomedical engineering. Prior studies [93–95] could be extended through optimizing feature selection and applying the computational of the fractal dimension and related parameters (e.g., lacunarity) to other neuroimaging modalities such as functional MR images, CT, and positron-emission tomography (PET). Zook and Iftekharuddin proposed integrating tumor subtypes, geometrical size, and the effect of noise when analyzing fractal dimensions [98]. Wardlaw et al. suggested the removal of cardiac and respiratory factors from the blood oxygen level–dependent (BOLD) signals to better identify tumor subregions of active metabolism [122]. Iftekharrudin et al. recommended future studies to improve discrimination of various brain tissues, i.e., white matter, gray matter, cerebrospinal fluid, and skull, in order to better distinguish solid tumors and areas of edema [58]. In the computational era, fractal-based analysis may be incorporated into diffusion tensor imaging studies and even nuclear medicine tools. For instance, fractal analysis of single photon emission computed tomography (SPECT) and PET imaging may deepen our insight of radiomics and may offer novel biomarkers that are clinically applicable [123].

Conclusion

With novel imaging biomarkers being uncovered at an accelerating rate through radiomics, comes a new frontier for integrating multiparametric data to improve the treatment of brain tumors. Computational models are expanding with the use of machine learning and fractal-based analysis, which are increasingly becoming paramount for diagnostic and prognostic accuracy. Over time, these models will have to be aligned with tumor biology to maximize the clinical implications of radiomics. Current obstacles in understanding tumor heterogeneity may be overcome through increased research in computational models and extending those findings to the clinical realm. Our review of the newly emerging radiomic techniques via machine learning and fractal-based analyses demonstrate the potential for improving diagnostic and prognostic accuracy of gliomas. The field of radiomics is a rapidly developing

field with many avenues yet to be explored for further discovery and innovation.

Acknowledgments Professor Antonio Di Ieva received the 2019 John Mitchell Crouch Fellowship from the Royal Australasian College of Surgeons (RACS) which, along with Macquarie University co-funding, supported the opening of the Computational NeuroSurgery (CNS) Lab at Macquarie University, Sydney, Australia. Moreover, he is supported by an Australian Research Council (ARC) Future Fellowship (2019-2023, FT190100623). KJ would like to personally thank Professor Antonio Di Ieva, Dr. Carlo Russo, and Dr. Abhishta Bhandari for their untiring support during the course of this work. We also thank Dr. Bhandari for contributing to the figure used in this manuscript.

Funding information No funding was received for this study.

Compliance with ethical standards

Conflict of interest The authors declare that they have no conflict of interest.

Ethical approval All procedures performed in the studies involving human participants were in accordance with the ethical standards of the institutional and/or national research committee and with the 1964 Helsinki Declaration and its later amendments or comparable ethical standards.

Informed consent Informed consent was obtained from all individual participants included in the study.

References

1. Gillies RJ, Kinahan PE, Hricak H (2016) Radiomics: images are more than pictures, they are data. Radiology 278(2):563–577. https://doi.org/10.1148/radiol.2015151169
2. Kumar V, Gu Y, Basu S, Berglund A, Eschrich SA, Schabath MB, Forster K, Aerts HJ, Dekker A, Fenstermacher D, Goldgof DB, Hall LO, Lambin P, Balagurunathan Y, Gatenby RA, Gillies RJ (2012) Radiomics: the process and the challenges. Magn Reson Imaging 30(9):1234–1248. https://doi.org/10.1016/j.mri.2012.06.010
3. Zhou M, Chaudhury B, Hall LO, Goldgof DB, Gillies RJ, Gatenby RA (2017) Identifying spatial imaging biomarkers of glioblastoma multiforme for survival group prediction. J Magn Reson Imaging 46(1):115–123. https://doi.org/10.1002/jmri.25497
4. Gutman DA, Cooper LA, Hwang SN, Holder CA, Gao J, Aurora TD, Dunn WD Jr, Scarpace L, Mikkelsen T, Jain R, Wintermark M, Jilwan M, Raghavan P, Huang E, Clifford RJ, Mongkolwat P, Kleper V, Freymann J, Kirby J, Zinn PO, Moreno CS, Jaffe C, Colen R, Rubin DL, Saltz J, Flanders A, Brat DJ (2013) MR imaging predictors of molecular profile and survival: multi-institutional study of the TCGA glioblastoma data set. Radiology 267(2):560–569. https://doi.org/10.1148/radiol.13120118
5. Kotrotsou A, Zinn PO, Colen RR (2016) Radiomics in brain tumors: an emerging technique for characterization of tumor environment. Magn Reson Imaging Clin N Am 24(4):719–729. https://doi.org/10.1016/j.mric.2016.06.006
6. Louis DN, Perry A, Reifenberger G, von Deimling A, Figarella-Branger D, Cavenee WK, Ohgaki H, Wiestler OD, Kleihues P, Ellison DW (2016) The 2016 World Health Organization classification of tumors of the central nervous system: a summary. Acta Neuropathol 131(6):803–820. https://doi.org/10.1007/s00401-016-1545-1
7. Bredel M, Scholtens DM, Harsh GR, Bredel C, Chandler JP, Renfrow JJ, Yadav AK, Vogel H, Scheck AC, Tibshirani R, Sikic BI (2009) A network model of a cooperative genetic landscape in brain tumors. JAMA 302(3):261–275. https://doi.org/10.1001/jama.2009.997
8. Sturm D, Witt H, Hovestadt V, Khuong-Quang D-A, Jones David TW, Konermann C, Pfaff E, Tönjes M, Sill M, Bender S, Kool M, Zapatka M, Becker N, Zucknick M, Hielscher T, Liu X-Y, Fontebasso Adam M, Ryzhova M, Albrecht S, Jacob K, Wolter M, Ebinger M, Schuhmann Martin U, van Meter T, Frühwald Michael C, Hauch H, Pekrun A, Radlwimmer B, Niehues T, von Komorowski G, Dürken M, Kulozik Andreas E, Madden J, Donson A, Foreman Nicholas K, Drissi R, Fouladi M, Scheurlen W, von Deimling A, Monoranu C, Roggendorf W, Herold-Mende C, Unterberg A, Kramm Christof M, Felsberg J, Hartmann C, Wiestler B, Wick W, Milde T, Witt O, Lindroth Anders M, Schwartzentruber J, Faury D, Fleming A, Zakrzewska M, Liberski Pawel P, Zakrzewski K, Hauser P, Garami M, Klekner A, Bognar L, Morrissy S, Cavalli F, Taylor Michael D, van Sluis P, Koster J, Versteeg R, Volckmann R, Mikkelsen T, Aldape K, Reifenberger G, Collins VP, Majewski J, Korshunov A, Lichter P, Plass C, Jabado N, Pfister Stefan M (2012) Hotspot mutations in H3F3A and IDH1 define distinct epigenetic and biological subgroups of glioblastoma. Cancer Cell 22(4):425–437. https://doi.org/10.1016/j.ccr.2012.08.024
9. Yan H, Parsons DW, Jin G, McLendon R, Rasheed BA, Yuan W, Kos I, Batinic-Haberle I, Jones S, Riggins GJ, Friedman H, Friedman A, Reardon D, Herndon J, Kinzler KW, Velculescu VE, Vogelstein B, Bigner DD (2009) IDH1 and IDH2 mutations in gliomas. N Engl J Med 360(8):765–773. https://doi.org/10.1056/NEJMoa0808710
10. Sanson M, Marie Y, Paris S, Idbaih A, Laffaire J, Ducray F, El Hallani S, Boisselier B, Mokhtari K, Hoang-Xuan K, Delattre J-Y (2009) Isocitrate dehydrogenase 1 codon 132 mutation is an important prognostic biomarker in gliomas. J Clin Oncol 27(25):4150–4154. https://doi.org/10.1200/JCO.2009.21.9832
11. Eckel-Passow JE, Lachance DH, Molinaro AM, Walsh KM, Decker PA, Sicotte H, Pekmezci M, Rice T, Kosel ML, Smirnov IV, Sarkar G, Caron AA, Kollmeyer TM, Praska CE, Chada AR, Halder C, Hansen HM, McCoy LS, Bracci PM, Marshall R, Zheng S, Reis GF, Pico AR, O'Neill BP, Buckner JC, Giannini C, Huse JT, Perry A, Tihan T, Berger MS, Chang SM, Prados MD, Wiemels J, Wiencke JK, Wrensch MR, Jenkins RB (2015) Glioma groups based on 1p/19q, IDH, and TERT promoter mutations in tumors. N Engl J Med 372(26):2499–2508. https://doi.org/10.1056/NEJMoa1407279
12. Jenkins RB, Blair H, Ballman KV, Giannini C, Arusell RM, Law M, Flynn H, Passe S, Felten S, Brown PD, Shaw EG, Buckner JC (2006) A t(1;19)(q10;p10) mediates the combined deletions of 1p and 19q and predicts a better prognosis of patients with oligodendroglioma. Cancer Res 66(20):9852–9861. https://doi.org/10.1158/0008-5472.CAN-06-1796
13. Hegi ME, Liu L, Herman JG, Stupp R, Wick W, Weller M, Mehta MP, Gilbert MR (2008) Correlation of O6-methylguanine methyltransferase (MGMT) promoter methylation with clinical outcomes in glioblastoma and clinical strategies to modulate MGMT activity. J Clin Oncol 26(25):4189–4199. https://doi.org/10.1200/JCO.2007.11.5964
14. Delfanti RL, Piccioni DE, Handwerker J, Bahrami N, Krishnan A, Karunamuni R, Hattangadi-Gluth JA, Seibert TM, Srikant A, Jones KA, Snyder VS, Dale AM, White NS, McDonald CR, Farid N (2017) Imaging correlates for the 2016 update on WHO

classification of grade II/III gliomas: implications for IDH, 1p/19q and ATRX status. J Neuro-Oncol 135(3):601–609. https://doi.org/10.1007/s11060-017-2613-7

15. Haas-Kogan DA, Prados MD, Tihan T, Eberhard DA, Jelluma N, Arvold ND, Baumber R, Lamborn KR, Kapadia A, Malec M, Berger MS, Stokoe D (2005) Epidermal growth factor receptor, protein kinase B/Akt, and glioma response to erlotinib. JNCI: J Natl Cancer Instit 97(12):880–887. https://doi.org/10.1093/jnci/dji161
16. Noushmehr H, Weisenberger DJ, Diefes K, Phillips HS, Pujara K, Berman BP, Pan F, Pelloski CE, Sulman EP, Bhat KP, Verhaak RGW, Hoadley KA, Hayes DN, Perou CM, Schmidt HK, Ding L, Wilson RK, Van Den Berg D, Shen H, Bengtsson H, Neuvial P, Cope LM, Buckley J, Herman JG, Baylin SB, Laird PW, Aldape K (2010) Identification of a CpG island methylator phenotype that defines a distinct subgroup of glioma. Cancer Cell 17(5):510–522. https://doi.org/10.1016/j.ccr.2010.03.017
17. Raab SS, Grzybicki DM, Janosky JE, Zarbo RJ, Meier FA, Jensen C, Geyer SJ (2005) Clinical impact and frequency of anatomic pathology errors in cancer diagnoses. Cancer 104(10):2205–2213. https://doi.org/10.1002/cncr.21431
18. Gerlinger M, Rowan AJ, Horswell S, Math M, Larkin J, Endesfelder D, Gronroos E, Martinez P, Matthews N, Stewart A, Tarpey P, Varela I, Phillimore B, Begum S, McDonald NQ, Butler A, Jones D, Raine K, Latimer C, Santos CR, Nohadani M, Eklund AC, Spencer-Dene B, Clark G, Pickering L, Stamp G, Gore M, Szallasi Z, Downward J, Futreal PA, Swanton C (2012) Intratumor heterogeneity and branched evolution revealed by multiregion sequencing. N Engl J Med 366(10):883–892. https://doi.org/10.1056/NEJMoa1113205
19. Friedmann-Morvinski D (2014) Glioblastoma heterogeneity and cancer cell plasticity. Crit Rev Oncog 19(5):327–336. https://doi.org/10.1615/critrevoncog.2014011777
20. Inda MM, Bonavia R, Seoane J (2014) Glioblastoma multiforme: a look inside its heterogeneous nature. Cancers (Basel) 6(1):226–239. https://doi.org/10.3390/cancers6010226
21. Gevaert O, Mitchell LA, Achrol AS, Xu J, Echegaray S, Steinberg GK, Cheshier SH, Napel S, Zaharchuk G, Plevritis SK (2014) Glioblastoma multiforme: exploratory radiogenomic analysis by using quantitative image features. Radiology 273(1):168–174. https://doi.org/10.1148/radiol.14131731
22. Zinn PO, Mahajan B, Sathyan P, Singh SK, Majumder S, Jolesz FA, Colen RR (2011) Radiogenomic mapping of edema/cellular invasion MRI-phenotypes in glioblastoma multiforme. PLoS One 6(10):e25451. https://doi.org/10.1371/journal.pone.0025451
23. Lambin P, Rios-Velazquez E, Leijenaar R, Carvalho S, van Stiphout RG, Granton P, Zegers CM, Gillies R, Boellard R, Dekker A, Aerts HJ (2012) Radiomics: extracting more information from medical images using advanced feature analysis. Eur J Cancer 48(4):441–446. https://doi.org/10.1016/j.ejca.2011.11.036
24. Djuricic GJ, Radulovic M, Sopta JP, Nikitovic M, Milosevic NT (2017) Fractal and gray level cooccurrence matrix computational analysis of primary osteosarcoma magnetic resonance images predicts the chemotherapy response. Front Oncol 7:246. https://doi.org/10.3389/fonc.2017.00246
25. Parekh V, Jacobs MA (2016) Radiomics: a new application from established techniques. Expert Rev Precis Med Drug Dev 1(2):207–226. https://doi.org/10.1080/23808993.2016.1164013
26. Haralick RM, Shanmugam K, Dinstein I (1973) Textural features of image classification. IEEE Trans Syst Man Cybern 3(6):610–621. https://doi.org/10.1109/TSMC.1973.4309314
27. Czarnek N, Clark K, Peters KB, Mazurowski MA (2017) Algorithmic three-dimensional analysis of tumor shape in MRI improves prognosis of survival in glioblastoma: a multi-institutional study. J Neuro-Oncol 132(1):55–62. https://doi.org/10.1007/s11060-016-2359-7
28. Mazurowski MA, Czarnek NM, Collins LM, Peters KB, Clark K (2016) Predicting outcomes in glioblastoma patients using computerized analysis of tumor shape - preliminary data. In: Progress in Biomedical Optics and Imaging - Proceedings of SPIE. https://doi.org/10.1117/12.2217098
29. Ditmer A, Zhang B, Shujaat T, Pavlina A, Luibrand N, Gaskill-Shipley M, Vagal A (2018) Diagnostic accuracy of MRI texture analysis for grading gliomas. J Neuro-Oncol 140(3):583–589. https://doi.org/10.1007/s11060-018-2984-4
30. Galloway MM (1975) Texture analysis using gray level run lengths. Comput Graphics Image Process 4(2):172–179. https://doi.org/10.1016/S0146-664X(75)800086
31. Amadasun M, King R (1989) Textural features corresponding to textural properties. IEEE Trans Syst Man Cybern 19(5):1264–1274. https://doi.org/10.1109/21.44046
32. Ojala T, Pietikäinen M, Mäenpää T (2002) Multiresolution gray-scale and rotation invariant texture classification with local binary patterns, vol 24. vol 7 %. J IEEE Trans Pattern Anal Mach. Intell. IEEE Computer Society. https://doi.org/10.1109/tpami.2002.1017623
33. Ambrosini RD, Wang P, O'Dell WG (2010) Computer-aided detection of metastatic brain tumors using automated three-dimensional template matching. J Magn Reson Imaging 31(1):85–93. https://doi.org/10.1002/jmri.22009
34. Lowe DG (1999) Object recognition from local scale-invariant features. In: Proceedings of the Seventh IEEE International Conference on Computer Vision, 20–27 Sept. 1999. pp 1150–1157 vol.1152. https://doi.org/10.1109/ICCV.1999.790410
35. Dalal N, Triggs B (2005) Histograms of oriented gradients for human detection. In: 2005 IEEE Computer Society Conference on Computer Vision and Pattern Recognition (CVPR'05), 20–25 June 2005. vol. 881. pp 886–893. https://doi.org/10.1109/CVPR.2005.177
36. Mandelbrot BB, Freeman WH, Company (1983) The fractal geometry of nature. Henry Holt and Company
37. Di Ieva A, Grizzi F, Jelinek H, Pellionisz AJ, Losa GA (2013) Fractals in the neurosciences, part I: general principles and basic neurosciences. Neuroscientist 20(4):403–417. https://doi.org/10.1177/1073858413513927
38. Di Ieva A, Esteban FJ, Grizzi F, Klonowski W, Martín-Landrove M (2013) Fractals in the neurosciences, part II: clinical applications and future perspectives. Neuroscientist 21(1):30–43. https://doi.org/10.1177/1073858413513928
39. Smitha KA, Gupta AK, Jayasree RS (2015) Fractal analysis: fractal dimension and lacunarity from MR images for differentiating the grades of glioma. Phys Med Biol 60(17):6937–6947. https://doi.org/10.1088/0031-9155/60/17/6937
40. Lim JS (1990) Two-dimensional signal and image processing. Prentice-Hall, Inc.
41. Gonzalez RC, Woods RE, Eddins SL (2004) Digital image processing using MATLAB. Pearson Education
42. Aerts HJ, Velazquez ER, Leijenaar RT, Parmar C, Grossmann P, Carvalho S, Bussink J, Monshouwer R, Haibe-Kains B, Rietveld D, Hoebers F, Rietbergen MM, Leemans CR, Dekker A, Quackenbush J, Gillies RJ, Lambin P (2014) Decoding tumour phenotype by noninvasive imaging using a quantitative radiomics approach. Nat Commun 5:4006. https://doi.org/10.1038/ncomms5006
43. van Griethuysen JJM, Fedorov A, Parmar C, Hosny A, Aucoin N, Narayan V, Beets-Tan RGH, Fillion-Robin JC, Pieper S, Aerts H (2017) Computational Radiomics system to decode the radiographic phenotype. Cancer Res 77(21):e104–e107. https://doi.org/10.1158/0008-5472.Can-17-0339

44. Rizzo S, Botta F, Raimondi S, Origgi D, Fanciullo C, Morganti AG, Bellomi M (2018) Radiomics: the facts and the challenges of image analysis. Eur Radiol Exp 2(1):36–36. https://doi.org/10.1186/s41747-018-0068-z
45. Earnest F, Kelly PJ, Scheithauer BW, Kall BA, Cascino TL, Ehman RL, Forbes GS, Axley PL (1988) Cerebral astrocytomas: histopathologic correlation of MR and CT contrast enhancement with stereotactic biopsy. Radiology 166(3):823–827. https://doi.org/10.1148/radiology.166.3.2829270
46. Zhou M, Scott J, Chaudhury B, Hall L, Goldgof D, Yeom KW, Iv M, Ou Y, Kalpathy-Cramer J, Napel S, Gillies R, Gevaert O, Gatenby R (2018) Radiomics in brain tumor: image assessment, quantitative feature descriptors, and machine-learning approaches. Am J Neuroradiol 39(2):208–216. https://doi.org/10.3174/ajnr.A5391
47. Gatenby RA, Grove O, Gillies RJ (2013) Quantitative imaging in cancer evolution and ecology. Radiology 269(1):8–15. https://doi.org/10.1148/radiol.13122697
48. Zhou M, Hall L, Goldgof D, Gillies R, Gatenby R (2013) Survival time prediction of patients with glioblastoma multiforme tumors using spatial distance measurement, vol 8670. SPIE Medical Imaging. SPIE
49. Cao Y, Tsien CI, Nagesh V, Junck L, Ten Haken R, Ross BD, Chenevert TL, Lawrence TS (2006) Survival prediction in high-grade gliomas by MRI perfusion before and during early stage of RT [corrected]. Int J Radiat Oncol Biol Phys 64(3):876–885. https://doi.org/10.1016/j.ijrobp.2005.09.001
50. Zhou M, Hall L, Goldgof D, Russo R, Balagurunathan Y, Gillies R, Gatenby R (2014) Radiologically defined ecological dynamics and clinical outcomes in glioblastoma multiforme: preliminary results. Transl Oncol 7(1):5–13. https://doi.org/10.1593/tlo.13730
51. Chang PD, Malone HR, Bowden SG, Chow DS, Gill BJA, Ung TH, Samanamud J, Englander ZK, Sonabend AM, Sheth SA, McKhann GM 2nd, Sisti MB, Schwartz LH, Lignelli A, Grinband J, Bruce JN, Canoll P (2017) A multiparametric model for mapping cellularity in glioblastoma using radiographically localized biopsies. AJNR Am J Neuroradiol 38(5):890–898. https://doi.org/10.3174/ajnr.A5112
52. Gordillo N, Montseny E, Sobrevilla P (2013) State of the art survey on MRI brain tumor segmentation. Magn Reson Imaging 31(8):1426–1438. https://doi.org/10.1016/j.mri.2013.05.002
53. Gibbs P, Buckley DL, Blackband SJ, Horsman A (1996) Tumour volume determination from MR images by morphological segmentation. Phys Med Biol 41(11):2437–2446. https://doi.org/10.1088/0031-9155/41/11/014
54. Hojjatoleslami SA, Kittler J (1998) Region growing: a new approach. IEEE Trans Image Process 7(7):1079–1084. https://doi.org/10.1109/83.701170
55. Mie S, Lakare S, Ming W, Kaufman A, Nakajima M (2000) A gradient magnitude based region growing algorithm for accurate segmentation. In: Proceedings 2000 International Conference on Image Processing (Cat. No.00CH37101), 10–13 Sept. 2000. vol.443, pp 448–451. https://doi.org/10.1109/ICIP.2000.899432
56. Dam E, Loog M, Letteboer M (2004) Integrating automatic and interactive brain tumor segmentation. In: Proceedings of the 17th International Conference on Pattern Recognition, 2004. ICPR 2004., 26–26 Aug. 2004. vol 793, pp 790–793. https://doi.org/10.1109/ICPR.2004.1334647
57. Kannan SR (2008) A new segmentation system for brain MR images based on fuzzy techniques. Appl Soft Comput 8(4):1599–1606. https://doi.org/10.1016/j.asoc.2007.10.025
58. Iftekharuddin KM, Zheng J, Islam MA, Ogg RJ (2009) Fractal-based brain tumor detection in multimodal MRI. Appl Math Comput 207(1):23–41. https://doi.org/10.1016/j.amc.2007.10.063
59. Bernal J, Kushibar K, Asfaw DS, Valverde S, Oliver A, Martí R, Lladó X (2019) Deep convolutional neural networks for brain image analysis on magnetic resonance imaging: a review. Artif Intell Med 95:64–81. https://doi.org/10.1016/j.artmed.2018.08.008
60. Zikic D, Ioannou Y, Brown M, Criminisi A (2014) Segmentation of brain tumor tissues with convolutional neural networks. In: Proceedings MICCAI-BRATS. pp 36–39
61. Brébisson Ad, Montana G (2015) Deep neural networks for anatomical brain segmentation. In: 2015 IEEE Conference on Computer Vision and Pattern Recognition Workshops (CVPRW), 7–12 June 2015. pp 20–28. https://doi.org/10.1109/CVPRW.2015.7301312
62. Havaei M, Davy A, Warde-Farley D, Biard A, Courville A, Bengio Y, Pal C, Jodoin P-M, Larochelle H (2017) Brain tumor segmentation with deep neural networks. Med Image Anal 35:18–31. https://doi.org/10.1016/j.media.2016.05.004
63. Zhang W, Li R, Deng H, Wang L, Lin W, Ji S, Shen D (2015) Deep convolutional neural networks for multi-modality isointense infant brain image segmentation. NeuroImage 108:214–224. https://doi.org/10.1016/j.neuroimage.2014.12.061
64. Lyksborg M, Puonti O, Agn M, Larsen R (2015) An ensemble of 2D convolutional neural networks for tumor segmentation. In: Paulsen RR, Pedersen KS (eds) Image Analysis, Cham, 2015. Springer International Publishing, p 201–211
65. Li W, Wang G, Fidon L, Ourselin S, Cardoso MJ, Vercauteren T (2017) On the compactness, efficiency, and representation of 3D convolutional networks: brain parcellation as a pretext task. In: Niethammer M, Styner M, Aylward S, et al (eds) Information Processing in Medical Imaging, Cham, 2017. Springer International Publishing, p 348–360
66. Kamnitsas K, Ledig C, Newcombe VFJ, Simpson JP, Kane AD, Menon DK, Rueckert D, Glocker B (2017) Efficient multi-scale 3D CNN with fully connected CRF for accurate brain lesion segmentation. Med Image Anal 36:61–78. https://doi.org/10.1016/j.media.2016.10.004
67. McInerney T, Terzopoulos D (1996) Deformable models in medical image analysis: a survey. Med Image Anal 1(2):91–108. https://doi.org/10.1016/S1361-8415(96)80007-7
68. Wu Y, Zhao Z, Wu W, Lin Y, Wang M (2019) Automatic glioma segmentation based on adaptive superpixel. BMC Med Imaging 19(1):73. https://doi.org/10.1186/s12880-019-0369-6
69. Madabhushi A, Udupa JK (2006) New methods of MR image intensity standardization via generalized scale. Med Phys 33(9):3426–3434. https://doi.org/10.1118/1.2335487
70. Di Ieva A, Matula C, Grizzi F, Grabner G, Trattnig S, Tschabitscher M (2012) Fractal analysis of the susceptibility weighted imaging patterns in malignant brain tumors during antiangiogenic treatment: technical report on four cases serially imaged by 7 T magnetic resonance during a period of four weeks. World Neurosurg 77(5-6):785.e711–785.e721. https://doi.org/10.1016/j.wneu.2011.09.006
71. Sottoriva A, Spiteri I, Piccirillo SGM, Touloumis A, Collins VP, Marioni JC, Curtis C, Watts C, Tavaré S (2013) Intratumor heterogeneity in human glioblastoma reflects cancer evolutionary dynamics. Proc Natl Acad Sci U S A 110(10):4009–4014. https://doi.org/10.1073/pnas.1219747110
72. Georgiadis P, Cavouras D, Kalatzis I, Glotsos D, Athanasiadis E, Kostopoulos S, Sifaki K, Malamas M, Nikiforidis G, Solomou E (2009) Enhancing the discrimination accuracy between metastases, gliomas and meningiomas on brain MRI by volumetric textural features and ensemble pattern recognition methods. Magn Reson Imaging 27(1):120–130. https://doi.org/10.1016/j.mri.2008.05.017
73. Yang D, Rao G, Martinez J, Veeraraghavan A, Rao A (2015) Evaluation of tumor-derived MRI-texture features for discrimination of molecular subtypes and prediction of 12-month survival

status in glioblastoma. Med Phys 42(11):6725–6735. https://doi.org/10.1118/1.4934373
74. Molina D, Perez-Beteta J, Luque B, Arregui E, Calvo M, Borras JM, Lopez C, Martino J, Velasquez C, Asenjo B, Benavides M, Herruzo I, Martinez-Gonzalez A, Perez-Romasanta L, Arana E, Perez-Garcia VM (2016) Tumour heterogeneity in glioblastoma assessed by MRI texture analysis: a potential marker of survival. Br J Radiol 89(1064):20160242. https://doi.org/10.1259/bjr.20160242
75. Chang K, Zhang B, Guo X, Zong M, Rahman R, Sanchez D, Winder N, Reardon DA, Zhao B, Wen PY, Huang RY (2016) Multimodal imaging patterns predict survival in recurrent glioblastoma patients treated with bevacizumab. Neuro-Oncology 18(12):1680–1687. https://doi.org/10.1093/neuonc/now086
76. Sanghani P, Ang BT, King NKK, Ren H (2018) Overall survival prediction in glioblastoma multiforme patients from volumetric, shape and texture features using machine learning. Surg Oncol 27(4):709–714. https://doi.org/10.1016/j.suronc.2018.09.002
77. Lao J, Chen Y, Li Z-C, Li Q, Zhang J, Liu J, Zhai G (2017) A deep learning-based radiomics model for prediction of survival in glioblastoma multiforme. Sci Rep 7(1):10353. https://doi.org/10.1038/s41598-017-10649-8
78. Li Q, Bai H, Chen Y, Sun Q, Liu L, Zhou S, Wang G, Liang C, Li Z-C (2017) A fully-automatic multiparametric radiomics model: towards reproducible and prognostic imaging signature for prediction of overall survival in glioblastoma multiforme. Sci Rep 7(1):14331. https://doi.org/10.1038/s41598-017-14753-7
79. Prasanna P, Patel J, Partovi S, Madabhushi A, Tiwari P (2017) Radiomic features from the peritumoral brain parenchyma on treatment-naive multi-parametric MR imaging predict long versus short-term survival in glioblastoma multiforme: preliminary findings. Eur Radiol 27(10):4188–4197. https://doi.org/10.1007/s00330-016-4637-3
80. Bahrami N, Piccioni D, Karunamuni R, Chang YH, White N, Delfanti R, Seibert TM, Hattangadi-Gluth JA, Dale A, Farid N, McDonald CR (2018) Edge contrast of the FLAIR hyperintense region predicts survival in patients with high-grade gliomas following treatment with bevacizumab. AJNR Am J Neuroradiol 39(6):1017–1024. https://doi.org/10.3174/ajnr.A5620
81. Bisdas S, Shen HC, Thust S, Katsaros V, Stranjalis G, Boskos C, Brandner S, Zhang JG (2018) Texture analysis- and support vector machine-assisted diffusional kurtosis imaging may allow in vivo gliomas grading and IDH-mutation status prediction: a preliminary study Scientific Reports 8. https://doi.org/10.1038/s41598-018-24438-4
82. Bae S, Choi YS, Ahn SS, Chang JH, Kang SG, Kim EH, Kim SH, Lee SK (2018) Radiomic MRI phenotyping of glioblastoma: improving survival prediction. Radiology 289(3):797–806. https://doi.org/10.1148/radiol.2018180200
83. Bahrami N, Hartman SJ, Chang YH, Delfanti R, White NS, Karunamuni R, Seibert TM, Dale AM, Hattangadi-Gluth JA, Piccioni D, Farid N, McDonald CR (2018) Molecular classification of patients with grade II/III glioma using quantitative MRI characteristics. J Neuro-Oncol 139(3):633–642. https://doi.org/10.1007/s11060-018-2908-3
84. Chaddad A, Sabri S, Niazi T, Abdulkarim B (2018) Prediction of survival with multi-scale radiomic analysis in glioblastoma patients. Med Biol Eng Comput 56(12):2287–2300. https://doi.org/10.1007/s11517-018-1858-4
85. Darbar A, Waqas M, Enam SF, Mahmood SD (2018) Use of preoperative apparent diffusion coefficients to predict brain tumor grade. Cureus 10(3):e2284. https://doi.org/10.7759/cureus.2284
86. Osman AFI (2019) A multi-parametric MRI-based radiomics signature and a practical ML model for stratifying glioblastoma patients based on survival toward precision oncology. Front Comput Neurosci 13:58. https://doi.org/10.3389/fncom.2019.00058
87. Petrujkic K, Milosevic N, Rajkovic N, Stanisavljevic D, Gavrilovic S, Dzelebdzic D, Ilic R, Di Ieva A, Maksimovic R (2019) Computational quantitative MR image features - a potential useful tool in differentiating glioblastoma from solitary brain metastasis. Eur J Radiol 119:108634. https://doi.org/10.1016/j.ejrad.2019.08.003
88. Yang Y, Yan LF, Zhang X, Nan HY, Hu YC, Han Y, Zhang J, Liu ZC, Sun YZ, Tian Q, Yu Y, Sun Q, Wang SY, Zhang X, Wang W, Cui GB (2019) Optimizing texture retrieving model for multimodal MR image-based support vector machine for classifying glioma. J Magn Reson Imaging 49(5):1263–1274. https://doi.org/10.1002/jmri.26524
89. Schoenegger K, Oberndorfer S, Wuschitz B, Struhal W, Hainfellner J, Prayer D, Heinzl H, Lahrmann H, Marosi C, Grisold W (2009) Peritumoral edema on MRI at initial diagnosis: an independent prognostic factor for glioblastoma? Eur J Neurol 16(7):874–878. https://doi.org/10.1111/j.1468-1331.2009.02613.x
90. Lacroix M, Abi-Said D, Fourney DR, Gokaslan ZL, Shi W, DeMonte F, Lang FF, McCutcheon I, Hassenbusch SJ, Holland E, Hess K, Michael C, Miller D, Sawaya R (2001) A multivariate analysis of 416 patients with glioblastoma multiforme: prognosis, extent of resection, and survival. J Neurosurg 95(2):190–198. https://doi.org/10.3171/jns.2001.95.2.0190
91. Skogen K, Schulz A, Dormagen JB, Ganeshan B, Helseth E, Server A (2016) Diagnostic performance of texture analysis on MRI in grading cerebral gliomas. Eur J Radiol 85(4):824–829. https://doi.org/10.1016/j.ejrad.2016.01.013
92. Macyszyn L, Akbari H, Pisapia JM, Da X, Attiah M, Pigrish V, Bi Y, Pal S, Davuluri RV, Roccograndi L, Dahmane N, Martinez-Lage M, Biros G, Wolf RL, Bilello M, O'Rourke DM, Davatzikos C (2016) Imaging patterns predict patient survival and molecular subtype in glioblastoma via machine learning techniques. Neuro-Oncology 18(3):417–425. https://doi.org/10.1093/neuonc/nov127
93. Lahmiri S, Boukadoum M (2012) Automatic brain MR images diagnosis based on edge fractal dimension and spectral energy signature. Conf Proc IEEE Eng Med Biol Soc 2012:6243–6246. https://doi.org/10.1109/embc.2012.6347421
94. Lahmiri S, Boukadoum M, Di Ieva A (2014) Detrended fluctuation analysis of brain hemisphere magnetic resonnance images to detect cerebral arteriovenousmalformations. In: 2014 IEEE International Symposium on Circuits and Systems (ISCAS), 1–5 June 2014. pp 2409–2412 https://doi.org/10.1109/ISCAS.2014.6865658
95. Lahmiri S, Boukadoum M (2013) Automatic detection of Alzheimer disease in brain magnetic resonance images using fractal features. In: 2013 6th International IEEE/EMBS Conference on Neural Engineering (NER), 6–8 Nov. 2013. p 1505–1508. https://doi.org/10.1109/NER.2013.6696231
96. Di Ieva A (Ed.) (2016) The fractal geometry of the brain. Springer, New York
97. Iftekharuddin KM, Jia W, Marsh R (2003) Fractal analysis of tumor in brain MR images. Mach Vis Appl 13(5):352–362. https://doi.org/10.1007/s00138-002-0087-9
98. Zook JM, Iftekharuddin KM (2005) Statistical analysis of fractal-based brain tumor detection algorithms. Magn Reson Imaging 23(5):671–678. https://doi.org/10.1016/j.mri.2005.04.002
99. Di Ieva A, Göd S, Grabner G, Grizzi F, Sherif C, Matula C, Tschabitscher M, Trattnig S (2013) Three-dimensional susceptibility-weighted imaging at 7 T using fractal-based quantitative analysis to grade gliomas. Neuroradiology 55(1):35–40. https://doi.org/10.1007/s00234-012-1081-1
100. Kristin RS, Alvord EC, Murray JD (2003) Dynamics of a model for brain tumors reveals a small window for therapeutic intervention. Discrete Contin Dynam Syst B 4(1):289–295. https://doi.org/10.3934/dcdsb.2004.4.289

101. Sedivy R (1996) Fractal tumours: their real and virtual images. Wien Klin Wochenschr 108(17):547–551
102. Di Ieva A (2010) Angioarchitectural morphometrics of brain tumors: are there any potential histopathological biomarkers? Microvasc Res 80(3):522–533. https://doi.org/10.1016/j.mvr.2010.09.005
103. Di Ieva A, Grizzi F, Ceva-Grimaldi G, Russo C, Gaetani P, Aimar E, Levi D, Pisano P, Tancioni F, Nicola G, Tschabitscher M, Dioguardi N, Baena RRY (2007) Fractal dimension as a quantitator of the microvasculature of normal and adenomatous pituitary tissue. J Anat 211(5):673–680. https://doi.org/10.1111/j.1469-7580.2007.00804.x
104. Di Ieva A, Grizzi F, Gaetani P, Goglia U, Tschabitscher M, Mortini P, Rodriguez y Baena R (2008) Euclidean and fractal geometry of microvascular networks in normal and neoplastic pituitary tissue. Neurosurg Rev 31(3):271–281. https://doi.org/10.1007/s10143-008-01277
105. Di Ieva A, Grizzi F, Tschabitscher M, Colombo P, Casali M, Simonelli M, Widhalm G, Muzzio PC, Matula C, Chiti A, Rodriguez y Baena R (2010) Correlation of microvascular fractal dimension with positron emission tomography [(11)C]-methionine uptake in glioblastoma multiforme: preliminary findings. Microvasc Res 80(2):267–273. https://doi.org/10.1016/j.mvr.2010.04.003
106. Di Ieva A, Bruner E, Widhalm G, Minchev G, Tschabitscher M, Grizzi F (2012) Computer-assisted and fractal-based morphometric assessment of microvascularity in histological specimens of gliomas. Sci Rep 2(1):429. https://doi.org/10.1038/srep00429
107. Bates DW, Saria S, Ohno-Machado L, Shah A, Escobar G (2014) Big data in health care: using analytics to identify and manage high-risk and high-cost patients. Health Aff 33(7):1123–1131. https://doi.org/10.1377/hlthaff.2014.0041
108. Abrol S, Kotrotsou A, Salem A, Zinn PO, Colen RR (2017) Radiomic phenotyping in brain cancer to unravel hidden information in medical images. Top Magn Reson Imaging 26(1):43–53. https://doi.org/10.1097/rmr.0000000000000117
109. Cancer Genome Atlas Research Network (2008) Comprehensive genomic characterization defines human glioblastoma genes and core pathways. Nature 455(7216):1061–1068. https://doi.org/10.1038/nature07385
110. Prior FW, Clark K, Commean P, Freymann J, Jaffe C, Kirby J, Moore S, Smith K, Tarbox L, Vendt B, Marquez G (2013) TCIA: an information resource to enable open science. Conf Proc IEEE Eng Med Biol Soc 2013:1282–1285. https://doi.org/10.1109/embc.2013.6609742
111. Kalpathy-Cramer J, Freymann JB, Kirby JS, Kinahan PE, Prior FW (2014) Quantitative imaging network: data sharing and competitive algorithmvalidation leveraging the cancer imaging archive. Transl Oncol 7(1):147–152. https://doi.org/10.1593/tlo.13862
112. Heilbrun ME (2013) Evaluating RadLex and real world radiology reporting: are we there yet? Acad Radiol 20(11):1327–1328. https://doi.org/10.1016/j.acra.2013.09.011
113. Tibshirani R (1996) Regression shrinkage and selection via the lasso. J R Stat Soc Ser B Methodol 58(1):267–288
114. Gevaert O, Xu J, Hoang CD, Leung AN, Xu Y, Quon A, Rubin DL, Napel S, Plevritis SK (2012) Non-small cell lung cancer: identifying prognostic imaging biomarkers by leveraging public gene expression microarray data–methods and preliminary results. Radiology 264(2):387–396. https://doi.org/10.1148/radiol.12111607
115. Shen W, Zhou M, Yang F, Dong D, Yang C, Zang Y, Tian J (2016) Learning from experts: developing transferable deep features for patient-level lung cancer prediction. In: Ourselin S, Joskowicz L, Sabuncu MR, Unal G, Wells W (eds) Medical Image Computing and Computer-Assisted Intervention – MICCAI 2016, Cham, 2016. Springer International Publishing, p 124–131
116. Mamoshina P, Vieira A, Putin E, Zhavoronkov A (2016) Applications of deep learning in biomedicine. Mol Pharm 13(5):1445–1454. https://doi.org/10.1021/acs.molpharmaceut.5b00982
117. Chu HH, Choi SH, Ryoo I, Kim SC, Yeom JA, Shin H, Jung SC, Lee AL, Yoon TJ, Kim TM, Lee S-H, Park C-K, Kim J-H, Sohn C-H, Park S-H, Kim IH (2013) Differentiation of true progression from pseudoprogression in glioblastoma treated with radiation therapy and concomitant temozolomide: comparison study of standard and high-b-value diffusion-weighted imaging. Radiology 269(3):831–840. https://doi.org/10.1148/radiol.13122024
118. Chang PD, Chow DS, Yang PH, Filippi CG, Lignelli A (2017) Predicting glioblastoma recurrence by early changes in the apparent diffusion coefficient value and signal intensity on FLAIR images. AJR Am J Roentgenol 208(1):57–65. https://doi.org/10.2214/ajr.16.16234
119. Ellingson BM, Cloughesy TF, Lai A, Nghiemphu PL, Mischel PS, Pope WB (2011) Quantitative volumetric analysis of conventional MRI response in recurrent glioblastoma treated with bevacizumab. Neuro-Oncology 13(4):401–409. https://doi.org/10.1093/neuonc/noq206
120. Zhou M, Hall LO, Goldgof DB, Russo R, Gillies RJ, Gatenby RA (2015) Decoding brain cancer dynamics: a quantitative histogram-based approach using temporal MRI. In: Progress in Biomedical Optics and Imaging - Proceedings of SPIE. https://doi.org/10.1117/12.2075545
121. Hygino da Cruz LC, Rodriguez I, Domingues RC, Gasparetto EL, Sorensen AG (2011) Pseudoprogression and pseudoresponse: imaging challenges in the assessment of posttreatment glioma. Am J Neuroradiol 32(11):1978–1985. https://doi.org/10.3174/ajnr.A2397
122. Wardlaw G, Wong R, Noseworthy MD (2008) Identification of intratumour low frequency microvascular components via BOLD signal fractal dimension mapping. Phys Med 24(2):87–91. https://doi.org/10.1016/j.ejmp.2008.01.006
123. Michallek F, Dewey M (2014) Fractal analysis in radiological and nuclear medicine perfusion imaging: a systematic review. Eur Radiol 24(1):60–69. https://doi.org/10.1007/s00330-013-2977-9